DMD Fast Forward. Published on April 9, 2010 as doi:10.1124/dmd.109.030361

P450-Mediated Bioactivation of the EGFR Inhibitor Erlotinib to a Reactive Electrophile

*Xiaohai Li, Theodore M. Kamenecka, and Michael D. Cameron**

Department of Molecular Therapeutics (MC), Translational Research Institute (XL, TMK, MC), Scripps Florida, The Scripps Research Institute, 130 Scripps Way, Jupiter, FL 33458, USA

a) **Running Title: Erlotinib bioactivation**

b) Corresponding Author: Michael D. Cameron

Scripps Florida, Department of Molecular Therapeutics, 130 Scripps Way, Jupiter, FL 33458, USA.

Telephone: 561-228-2223.

E-mail: cameron@scripps.edu

c)

Number of pages:	24 + figures and tables
Tables:	1
Figures:	8
References:	33
Words in abstract:	201
Words in introduction:	450
Words in discussion:	822

d) Non-standard abbreviations: Erlotinib, ERL; ACN, acetonitrile; CID, collision-induced dissociation; HLM, human liver microsomes; MRM, multiple reaction monitoring; EPI, enhanced product ion; IDA, information dependent acquisition; PI, precursor ion scan. DP, de-clustering potential; CE, collision energy; GSH, reduced glutathione

DMD Fast Forward. Published on April 9, 2010 as DOI: 10.1124/dmd.109.030361
This article has not been copyedited and formatted. The final version may differ from this version.

Abstract

The epidermal growth factor receptor (EGFR) tyrosine kinase inhibitor erlotinib is approved for treatment of non-small cell lung cancer. Numerous reports of erlotinib-associated toxicities are consistent with immune-mediated toxicity including drug-induced hepatitis, interstitial lung disease, Stevens-Johnson syndrome, and toxic epidermal necrolysis. While the mechanism of toxicity has not been established, we present evidence that reactive intermediates are formed during the metabolism of erlotinib, which can covalently conjugate to the cysteine group of the peptide-mimetic glutathione. Seven erlotinib-GSH conjugates were identified in incubations with hepatic microsomes. Cytochrome P450-dependent adducts are proposed to be formed via reactive epoxide and electrophilic quinone-imine intermediates. In incubations of human liver microsomes, intestinal microsomes, pulmonary microsomes and recombinant P450s, CYP3A4 was the primary enzyme responsible for the bioactivation of erlotinib; however, CYP1A1, CYP1A2, CYP3A5, and CYP2D6 were capable of catalyzing the bioactivation as well. During the metabolism of erlotinib, CYP3A4 and CYP3A5 are irreversibly inactivated by erlotinib in a time- and concentration-dependent manner. Inactivation was not dependent upon oxidation of the erlotinib alkyne group to form a reactive oxirene or ketene, demonstrated by synthesizing analogs where the alkyne was replaced with a cyano group. CYP1A1, CYP1A2, and CYP2D6 were not inactivated despite catalyzing the formation of erlotinib-glutathione adducts.

DMD Fast Forward. Published on April 9, 2010 as DOI: 10.1124/dmd.109.030361
This article has not been copyedited and formatted. The final version may differ from this version.

Introduction

Erlotinib (ERL) is a reversible inhibitor of the epidermal growth factor receptor tyrosine kinase (HER1/EGFR), and was approved for the second- and third-line treatment of non-small cell lung cancer in 2005 (Siegel-Lakhai et al., 2005). Clinical trials indicate that erlotinib provides a survival benefit after failure of first line or second line chemotherapy as a single agent and in the treatment of advanced pancreatic adenocarcinomas together with chemotherapy (Tang et al., 2006; Moore et al., 2007). While having therapeutic benefit, treatment with erlotinib has been associated with life-threatening adverse effects including drug-induced hepatitis (Liu et al., 2007b; Ramanarayanan and Scarpace, 2007; Saif, 2008; Pellegrinotti et al., 2009), interstitial lung disease (Liu et al., 2007a; Makris et al., 2007), and the severe skin disorders Stevens-Johnson syndrome and toxic epidermal necrolysis (Chou et al., 2006; Lubbe et al., 2008; Bovenschen and Alkemade, 2009). In September 2008, OSI Pharmaceuticals and Genentech reported a pharmacokinetic study of 15 patients with advanced solid tumors and moderate liver impairment. Associated with the trial, 1 patient died from hepatorenal syndrome and another died because of progressive liver failure (OSI Pharmaceuticals and Genentech, 2008), with both deaths attributed to erlotinib.

In humans, erlotinib is extensively metabolized, predominantly by CYP3A4, and to a lesser extent by CYP1A2 and the inducible isoform CYP1A1 (Ling et al., 2006; Li et al., 2007), with metabolites excreted by the biliary system (~75%). There are three primary routes of erlotinib metabolism: O-demethylation of the side chain with/or without further oxidation to the carboxylic acid, oxidation of the acetylene moiety followed by further hydrolysis to the aryl carboxylic acid, and 4-hydroxylation of the phenyl-acetylene moiety (Ling et al., 2006). 4-hydroxylation forms a *para*-hydroxylated metabolite on the phenyl ring, resulting in the

formation of a *para*-hydroxyaniline (Li et al., 2007), which has the potential to undergo P450-mediated two electron oxidation to form a reactive quinine-imine.

In this study, we have monitored quinone-imine formation using GSH trapping. Compounds capable of reacting with GSH would be expected to be able to react with other cellular sulfhydrals such as in cysteine residues of protein. To date, erlotinib has not been reported to be metabolized to form reactive intermediates capable of reacting with biomolecules. We have demonstrated the formation of GSH adducts during the oxidative metabolism of erlotinib, have determined the site of bioactivation, and identified the individual human cytochrome P450 enzymes involved. Erlotinib was also found to inactivate CYP3A4 and CYP3A5 in a time- and concentration-dependent manner whereas CYP1A1 and CYP2D6 were not inactivated despite these enzymes forming glutathione-reactive metabolites. Finally we demonstrated that adduct formation and enzyme inactivation were not dependent on oxidation of the acetylene using synthesized erlotinib analogs where ethyl and cyano groups replaced the acetylene.

DMD Fast Forward. Published on April 9, 2010 as DOI: 10.1124/dmd.109.030361
This article has not been copyedited and formatted. The final version may differ from this version.

Materials and Methods

Materials

Pooled human liver microsomes, human intestinal microsomes, human pulmonary microsomes (smoker and non-smoker), and recombinant P450 + reductase bactosomes were purchased from XenoTech LLC (Lenexa, KS, USA). Recombinant human microsomal epoxide hydrolase was purchased from BD Gentest (Woburn, MA, USA). Formic acid, DMSO, and acetonitrile were purchased from Fisher Scientific (Fair Lawn, NJ). Erlotinib was purchased from LC Laboratories (Woburn, MA, USA). Midazolam, carbamazepine, α-naphthoflavone, phenacetin, diclofenac, (*S*)-mephenytoin, and ketoconazole were from Sigma-Aldrich (St. Louis, MO).

Analytical conditions.

LC-MS/MS analyses of GSH adducts were performed on an API 4000 Q-Trap mass spectrometer equipped with a Turboionspray source (Applied Biosystems, Foster City, CA), utilizing a negative precursor ion (PI) scan of *m/z* 272 (Dieckhaus et al., 2005), using conditions previously described (Li et al., 2009). Chromatographic separation was achieved by using an Agilent Eclipse XDB C18 column (3.5 µ, 3.0 × 150 mm). HPLC conditions used a flow rate of 0.4 ml/min with mobile phase A, water with 0.1% formic acid, and mobile phase B, acetonitrile with 0.1% formic acid. A gradient elution was utilized starting with 5% solvent B for 3 min, then solvent B was rapidly ramped to 10% in 0.5min, followed by 10-50% B in 19.5 min and 50-80% B in 5 min. At 28 min, the column was flushed with 80% B for 2 min and re-equilibrated to initial conditions. Structural information was generated from collision-induced dissociation (CID) spectra. Metabolites and GSH adducts were verified by comparing incubated samples to control samples without NADPH, trapping agent, or substrate.

To improve detection sensitivity and specificity, metabolites and GSH adducts were also characterized using multiple reaction monitoring triggered enhanced product ion scans (MRM-

DMD Fast Forward. Published on April 9, 2010 as DOI: 10.1124/dmd.109.030361
This article has not been copyedited and formatted. The final version may differ from this version.

IDA-EPI) following preset MRM transitions. The MRM transitions were set to the most intense ion pairs for each adduct, *m/z* 701.3→428.2, 715.3→442.2, and 717.3→444.2, with the following source settings: DP (70 V), CE (40 eV), and collision energy spread (±20 eV). The hydroxylaniline metabolite of erlotinib was followed using *m/z* 410.2→294.1 and carbamazepine (*m/z* 237.3→194.2) was used as an internal standard.

NMR analysis was recorded on a Bruker AV-400 NMR (Bruker AXS Inc. Madison, WI) in deuterated DMSO, and high resolution mass spectrometry was performed on an Orbitrap mass spectrometer (Thermo Fisher Scientific, San Jose, CA).

Microsomal incubations.

Pooled HLMs and recombinant P450 were thawed on ice. Erlotinib (40 μM from a DMSO stock) was mixed with HLM or recombinant enzyme (2 mg/ml protein for microsomes or 100 pmol/ml for recombinant P450) in 100 mM potassium phosphate buffer, pH 7.4, fortified with 5 mM GSH. The final concentration of organic solvent in the incubations was 0.2% (v/v). Incubations were performed at 37°C in a shaking incubator. After a 4 min pre-incubation at 37°C, reactions were initiated by the addition of 1 mM NADPH. Reactions were stopped by the addition of an equal volume of ACN (with or without I.S. added depending on analysis purpose) after 60 min. Control samples containing no NADPH or substrate, or control samples with heat-denatured HLM or blank phosphate buffer were included. Where indicated, ketoconazole (selective CYP3A4/5 inhibitor) was added at a final concentration of 1 μM, α-naphthoflavone (CYP1A1/2 inhibitor) at 20 μM, or microsomal epoxide hydrolase at 1 mg/ml were added to the incubations. Samples were centrifuged at 10,000 x *g* for 10 min at 4°C to pellet proteins, and supernatants were dried down by SpeedVac and reconstituted in 100 μL 30% ACN.

DMD Fast Forward. Published on April 9, 2010 as DOI: 10.1124/dmd.109.030361
This article has not been copyedited and formatted. The final version may differ from this version.

Time- and concentration-dependent inactivation of P450s.

Time- and concentration-dependent loss of CYP3A4 activity in the presence of erlotinib was determined by midazolam 1'-hydroxylase activity. Primary incubations included erlotinib (0, 5, 10, 20, and 40 µM), 1 mM NADPH, 0.5 mg/ml HLM, 3 mM $MgCl_2$, and 0.1 M potassium phosphate buffer (pH 7.4). The mixture was incubated in a 37°C shaking incubator for various time points (0, 4, 8, 15, 22, and 30 min). At each pre-incubation time point, aliquots (10 µl) of the primary incubation mixtures were transferred to a secondary incubation with a final volume of 200 µl, Secondary incubations had a final concentration of 20 µM midazolam, 1 mM NADPH, 3 mM $MgCl_2$, and 0.1 M potassium phosphate (pH 7.4), and were incubated at 37°C for 5 min and stopped by the addition of acetonitrile (1:1 v:v). All the samples were analyzed as previously described (Li et al., 2009). Other major cytochrome P450s: CYP1A1, 1A2, 2D6, 2C9 and 2C19 were similarly evaluated according to validated assays (Perloff et al., 2009) with slight modification.

Nonspecific binding was evaluated by determining the percent unbound erlotinib under incubation conditions. Protein concentrations were chosen to reflect those for the primary incubations in the time dependent inactivation studies. Erlotinib concentrations were similar to the experimentally determined K_i (HLM, 20µM; recombinant CYP3A4, 10µM; and recombinant 3A5, 40µM). Erlotinib and enzyme were allowed to incubate 37°C for 20 min. Triplicate samples were centrifuged at 100,000 rpm (436,000 x g) in a Beckman Coulter TLA-120.2 rotor for 240 min at 4°C. Unbound erlotinib was determined by sampling 1-2 mm below the supernatant surface and comparing erlotinib levels to uncentrifuged samples.

Purification of *para*-hydroxyerlotinib.

Para-hydroxyerlotinib was purified from 1 ml incubations of human liver microsomes (1 mg/ml) containing 40 µM erlotinib, and 1 mM NADPH in a final volume of 1 ml. The reaction was

DMD Fast Forward. Published on April 9, 2010 as DOI: 10.1124/dmd.109.030361
This article has not been copyedited and formatted. The final version may differ from this version.

stopped after 1 hour by addition of 150 µL 10% trichloroacetic acid. Metabolites were isolated by solid phase extraction (Strata C18-E, 300 mg/3mL cartridges, Phenomenex) and further purified by manual collection of HPLC peaks.

Plasma and tissue concentration after oral dosing of erlotinib.

Tissue distribution of erlotinib was evaluated in C57Bl6 mice (n=3) dosed orally with erlotinib, 10 mg/kg. After two hours, blood, liver, lung, and brain were collected. Tissues were not perfused to reduce the risk that erlotinib would be eluted from the tissue during the perfusion process. Plasma was generated using standard centrifugation techniques and the plasma and tissues were frozen at -80˚C. Plasma and tissues were mixed with acetonitrile (1:5 v:v or 1:5 w:v, respectively), sonicated with a probe tip sonicator, and analyzed for drug levels by LC-MS/MS. All procedures were conducted in the Scripps vivarium, which is fully AAALAC accredited, and were approved by the Scripps Florida IACUC.

Synthesis of Erlotinib analogs.

Erlotinib analogs were prepared using the following general protocol. A mixture of aniline (3-ethyl aniline or 3-cyanoaniline) and commercially available 4-chloro-6,7-dimethoxyquinazoline (american Custom Chemical Corp.) were heated in isopropanol at 90˚C overnight. After cooling to 25C, the precipitates were filtered, washed with isopropanol, ether, and dried in vacuo to give the products as near colorless solids, >95% pure as judged by analytical HPLC and LC/MS analysis. Products were confirmed by 1H-NMR analysis.

DMD Fast Forward. Published on April 9, 2010 as DOI: 10.1124/dmd.109.030361
This article has not been copyedited and formatted. The final version may differ from this version.

Results

Erlotinib tissue distribution.

The major site of erlotinib metabolism is the liver. When dosed in mice, erlotinib concentrations were three-fold higher in the liver compared to the plasma. Lung concentrations did not show compound accumulation and brain levels are significantly below the level in plasma, **Table 1**. With standard therapy, daily 150 mg oral dose, the clinical erlotinib C_{max} is 6 to 8 µM (Rudin et al., 2008). If the liver to plasma ratio measured in mouse is representative of human, concentrations of 15 to 25 µM would be expected in the liver and higher levels may be observed in select individuals, including those with hepatic impairment or in patients taking medication that inhibit CYP3A. Most of the experiments presented in this study were conducted using 20 or 40 µM erlotinib.

Time- and concentration-dependent inactivation of P450 by erlotinib.

Preliminary experiments were conducted to investigate time-dependent inhibition of individual P450s in human liver microsomes by 80 µM erlotinib. Assessment of remaining P450 activity after 30 minutes showed that CYP3A4/5 activity was sharply decreased during the 30 minute incubation with erlotinib, whereas, CYP1A2, CYP2D6, CYP2C9 and CYP2C19 activities were essentially unchanged. More extensive experiments were carried out to evaluate the kinetics of CYP3A4/5 inactivation in human liver microsomes by erlotinib. Midazolam 1´-hydroxylation was used as a measure of CYP3A4/5 activity. As shown in **Fig.1A**, pre-incubation of erlotinib with HLM in the presence of NADPH decreased CYP3A4/5 activity in a time- and concentration-dependent manner. The observed first-order rate constants (k_{obs}) of the inactivation reaction were calculated for specific erlotinib concentrations. The hyperbolic plot of k_{obs} versus erlotinib concentrations is shown **in Fig.1B**. The k_{inact} was calculated to be 0.09 min^{-1} and K_I was 22 µM. Parallel incubations were setup where erlotinib was pre-incubated with

DMD Fast Forward. Published on April 9, 2010 as DOI: 10.1124/dmd.109.030361
This article has not been copyedited and formatted. The final version may differ from this version.

CYP3A4 in the absence of NADPH. No inactivation was observed in the absence of NADPH, and CYP3A4/5 activity was not protected by the presence of 5 mM glutathione or catalase/superoxide dismutase, Fig.1C. The reversibility of time-dependent inhibition was assessed by dialysis. Erlotinib incubations with HLM +/- NADPH were sampled at 0 and 20 minutes and 150 µl aliquots were dialyzed against 2L phosphate buffer (0.1 M, pH 7.4) for approximately 8 hours (fresh buffer at 4 hr) at 4°C with constant stirring. Pre- and post-dialysis CYP3A4/5 activity was determined for all conditions using midazolam hydroxylation as a marker for CYP3A4/5 activity. CYP3A4/5 activity was not recoverable by dialysis (data not shown).

Recombinant CYP3A4, 3A5, and 1A1 were utilized to further assess erlotinib-induced P450 inactivation. Recombinant CYP3A4 was inactivated and had similar kinetic constants as observed in human liver microsomes, k_{inact} = 0.10 min^{-1} and K_I = 9 µM. CYP3A5 inactivation was more complicated and appeared to have two phases. The initial phase corresponded to k_{inact} = 0.18 min^{-1} and K_I = 40 µM, but at approximately 30% remaining activity, the rate of inactivation was greatly decreased despite more than 70% of the initial erlotinib concentration remaining. CYP1A1 showed no evidence of inactivation.

Nonspecific binding was determined under conditions similar to the primary time-dependent incubations for HLM, recombinant CYP3A4 and CYP3A5 with erlotinib concentrations approximately equal to the determined K_I, 20, 10 and 40 µM, respectively. The fraction of free erlotinib was 12% for HLM, 14% for rCYP3A5, and 35% for rCYP3A4.

GSH adducts of erlotinib.

Glutathione was used as a representative cellular nucleophile. Seven GSH adducts were identified in NADPH supplemented HLM incubations containing erlotinib and GSH, as shown in **Fig.2A**. Four of the adducts were generated by cytochrome P450 and were NADPH

dependent, whereas three adducts (ERL-G3, G4, and G6) were also detected in control incubations and even when erlotinib and its metabolites were incubated with glutathione in buffer, **Fig.2B**.

Identification of enzyme-dependent ERL-GSH adducts.

Four erlotinib-GSH adducts, ERL-G1 (*m/z* 715.3), ERL-G2 (*m/z* 701.3), ERL-G5 (*m/z* 715.3), and ERL-G7 (*m/z* 715.3) were detected in incubations containing HLM and NADPH, but were not identified in control incubations suggesting these adducts were derived from NADPH-dependent bioactivation of erlotinib. Three of these adducts had *m/z* of 715.3 and all of had similar fragmentation patterns. The spectrum for the most abundant adduct, ERL-G5, is shown in **Fig.3**. The molecular ion of *m/z* 715.3 is consistent with attachment of the glutathionyl moiety to the monoxygenated metabolite of erlotinib (erlotinib+GSH+O-2H). Characteristic -129 Da fragments, resulting from the neutral loss of pyroglutamate were observed for all adducts. The major GSH adduct, ERL-G5 had a molecular ion of mass 715.241, which is consistent with the mass of the proposed metabolite ion, 715.240 (data not shown). Previous *in vitro* and human clinical studies report a major *para*-hydroxylated metabolite (Ling et al., 2006) and the three monohydroxylated-glutathione adducts are likely due to displacement of the three aromatic hydrogen.

ERL-G2 had a molecular ion of mass 701.3 and is proposed to be a demethylated secondary metabolite related to adducts G1, G5, and G7. While only one peak was detected, it is likely that there are demethylated secondary metabolites of all the GSH adducts. It is possible that some of the secondary metabolites were below the level of detection or they were not chromatographically resolved.

Identification of erlotinib-GSH adducts independent of enzyme and NADPH.

DMD Fast Forward. Published on April 9, 2010 as DOI: 10.1124/dmd.109.030361
This article has not been copyedited and formatted. The final version may differ from this version.

Two adducts, ELR-G3 (m/z 717.3) and ELR-G6 (m/z 701.3) were identified in incubated and control incubations without NADPH or when the microsomes were heat-inactivated by boiling for ten minutes. The molecular ion of ERL-G6, m/z 701.3, suggested the direct addition of GSH (erlotinib+GSH) and high resolution mass spectroscopy found a mass of m/z 701.263, which is consistent with the theoretical m/z 701.262, data not shown. Sample processing methods had an obvious effect on the formation of enzyme-independent adducts. If samples containing erlotinib and glutathione were directly concentrated using a SpeedVac, the amount of adduct was significantly higher than in samples where the concentration of glutathione was depleted by solid phase extraction prior to SpeedVac (data not shown). Similarly, overnight incubation of 4 mg/mL erlotinib and 200 mM GSH at 37°C in the absence of enzyme resulted in the formation of a GSH-erlotinib adduct with identical mass and retention time as ERL-G6 in sufficient quantities for an H-NMR spectrum, **Fig.4**. Glutathione appeared to be covalently conjugated to the alkyne group forming cis/trans isomers which lead to extensive splitting of the vinyl protons (the NMR signal for the alkyne hydrogen of unconjugated erlotinib is a singlet). A second GSH-erlotinib adduct consistent with ELR-G3, m/z 717.3, (erlotinib+GSH+O) may be due to oxidation of the sulfur of the attached glutathionyl moiety, but levels of ERL-G3 were too low for NMR analysis.

While ERL-G6 and –G3 could be formed in the absence of enzyme and NADPH, both adducts were formed in greater amounts when enzyme and NADPH were included in the incubation. This was particularly true with recombinant P450s. This may be due to a non-specific free radical reaction because addition of superoxide dismutase/catalase inhibited the formation of this adduct, showed in **Fig.5**. It is unclear if the alkyne group of erlotinib would react with nucleophiles in a biological setting or if this is an *in vitro* artifact.

DMD Fast Forward. Published on April 9, 2010 as DOI: 10.1124/dmd.109.030361
This article has not been copyedited and formatted. The final version may differ from this version.

The final detected adduct, ERL-G4, was formed through the non-enzymatic conjugation of glutathione to hydroxylated erlotinib. This was verified by incubating erlotinib with HLM and NADPH and isolating the metabolites by solid phase extraction. Addition of glutathione to the metabolites resulted in an adduct with the same mass and elution time as ERL-G4, **Fig.2B**.

Identification of the P450 enzymes responsible for erlotinib bioactivation in human microsomes.

ERL-G5 was the predominant enzyme-catalyzed GSH adduct. For simplicity, only ERL-G5 is shown in the phenotyping studies, but similar trends were seen with all three of the primary adducts. Bactosomes prepared from *Escherichia coli* membranes coexpressing recombinant human P450 and P450 reductase were utilized. As shown in **Fig.6A**, CYP3A4 had the highest level of ERL-G5 formation in incubations containing 100 pmol/mL recombinant P450 and 40 μM erlotinib. Adduct formation by CYP1A1 was approximately 36% of CYP3A4. CYP2D6, CYP3A5, and CYP1A2 also catalyzed ERL-G5 formation but the levels of adduct formation range from 9% to 16% of that formed by CYP3A4.

Based upon the results from recombinant P450 experiments, selective inhibitors of CYP1A1/2 and CYP3A4/5, α-naphathoflavone and ketoconazole, respectively, were evaluated in human hepatic, intestinal, and pulmonary microsome (smoker and non-smoker). As shown in **Fig.7A**, the addition of ketoconazole decreased ERL-G5 formation by 69 and 76 percent in liver and intestinal microsomes, but had no effect in pulmonary microsomes. While CYP3A4 appears to be the predominant catalyst of erlotinib bioactivation in the liver and intestine, other enzymes are likely responsible for 20 to 40% of adduct formation. The formation of ERL-G5 in pulmonary microsomes was low, but there was a large difference between smokers and non-smokers. CYP1A1/2 are likely to be the major enzymes responsible for erlotinib bioactivation in

DMD Fast Forward. Published on April 9, 2010 as DOI: 10.1124/dmd.109.030361
This article has not been copyedited and formatted. The final version may differ from this version.

the lung as the addition of the CYP1A1/2 inhibitor α-naphathoflavone inhibited ERL-G5 formation by 54 percent, **Fig.7B.**

Mechanism of P450-dependent formation of erlotinib-glutathione adducts.

Based upon the detected glutathione adducts, bioactivation is likely to proceed through the formation of a reactive epoxide and/or through the formation of a quinone-imine. To test this hypothesis, recombinant human microsomal epoxide hydrolase was added to reactions containing human liver microsomes or recombinant P450 with erlotinib, glutathione, and NADPH. The formation of ERL-G5 decreased by 35%, 55%, and 47% in incubations of human liver microsomes, and recombinant CYP3A4 and CYP1A1, respectively, **Fig.8**. Similar results were observed for other P450-dependent adducts. The addition of recombinant human microsomal epoxide hydrolase did not decrease the activity of CYP1A1/2 and CYP3A4/5 assayed by phenacetin demethylation and midazolam hydroxylation, respectively (data not shown).

Formation of *para*-hydroxyerlotinib (*para* hydroxylation on the aromatic aniline ring) was published by Ling *et al.* (Ling et al., 2006) (metabolite M16). This metabolite was determined to be the major metabolite in human plasma and accounted for approximately 10% of the total excreted dose (Ling et al., 2006). The two-electron oxidation of the *para*-hydroxyaniline moiety would generate a quinone-imine, which is electrophilic and can potentially react with cellular nucleophiles. A positive correlation (Pearson r = 0.85) was found between generation of *para*-hydroxyerlotinib and erlotinib-GSH adducts, **Fig. 6B.**

Hydroxyerlotinib was purified from microsomal incubations and used in reactions with recombinant P450 to test if CYP3A4 and CYP1A1 are capable of oxidizing the hydroxyerlotinib to form a quinone-imine (as seen during the oxidation of acetaminophen (Dahlin et al., 1984)). Similar mono-hydroxylated glutathione adducts were found with hydroxyerlotinib as with

DMD Fast Forward. Published on April 9, 2010 as DOI: 10.1124/dmd.109.030361
This article has not been copyedited and formatted. The final version may differ from this version.

erlotinib. If the formation of an epoxide was prerequisite for adduct formation, the observed adduct would be expected to incorporate an additional oxygen and be detected as a di-hydroxylated adduct.

N-Acetyl-lysine trapping.

N-Acetyl lysine is better suited to trap hard electrophiles that may be produced through oxidation of the alkyne group (oxirene and ketene intermediates). No N-acetyl-lysine-erlotinib adducts were detected.

Erlotinib Analogs.

To evaluate the role of the alkyne group in GSH adduct formation and in P450 inactivation, two analogs were synthesized. The alkyne group was replaced by an ethyl and a cyano group. Both analogs formed glutathione adducts in a P450 and NADPH dependent manner. The addition of 1 μM ketoconazole inhibited the formation of glutathione adducts by 90% and 97% for the ethyl and cyano analogs, respectively, indicating that CY3A4/5 was primarily responsible for adduct formation in HLM. The cyano analog was found to inactivate CYP3A4 in a time and concentration dependent manner with a K_I approximately 4 times higher than erlotinib (K_I = 78.4 μM and k_{inact} = 0.063 min^{-1}). CYP3A4 inactivation was not observed for the ethyl analog.

DMD Fast Forward. Published on April 9, 2010 as DOI: 10.1124/dmd.109.030361
This article has not been copyedited and formatted. The final version may differ from this version.

Discussion

CYP3A4, CYP3A5, and to a lesser degree CYP1A1 and CYP1A2 had been previously implicated in the metabolism of erlotinib (Ling et al., 2006; Li et al., 2007). The current study demonstrates that these same enzymes are capable of the metabolic bio-activation of erlotinib to form a reactive intermediate, capable of covalently binding to cellular nucleophiles. In addition to potential toxicity associated with covalent adduction of erlotinib to biomolecules, pharmacokinetic drug-drug interactions may be caused due to the inactivation of CYP3A4 and CYP3A5 during the metabolism of erlotinib.

Smoking has been shown to have a large effect on oral erlotinib pharmacokinetics. Smokers required 300 mg erlotinib to achieve similar C_{max} and AUC to non-smokers given a 150 mg dose (Hamilton et al., 2006). Tobacco smoke has been shown to increase the level of CYP1A1 mRNA and protein in human liver and lung (Hukkanen et al., 2002; Thum et al., 2006). The increased expression of CYP1A1 in the lungs of smokers may increase their risk of erlotinib associated interstitial lung disease. While we are not aware of a study examining the rates of interstitial lung disease in smokers vs. non-smokers being treated with erlotinib, there seems to be a relationship between smoking and interstitial lung disease with the structurally related drug gefitinib (Takano et al., 2004).

The proposed mechanism for the formations of erlotinib-GSH adducts is depicted in **Scheme 1**. The oxidation of erlotinib by P450 appears to form an epoxide that can react with nucleophiles such as the sulfhydral group of cysteine. An additional route of adduct formation is through the generation of a reactive quinone-imine (reactive intermediate associated with acetaminophen). A quinone-imine can be generated by oxidation of *para*-hydroxyerlotinib. In this study we found that CYP1A1 and CYP3A4 could oxidize hydroxyerlotinib to catalyze the formation of erlotinib-glutathione adducts, presumably through forming a quinone-imine; however, other

cellular oxidases may also be able to catalyze this reaction. While reactive epoxides and quinone-imine metabolites cannot diffuse significant distances from the organ where they were formed, *para*-hydroxyerlotinib is in general circulation and is the major erlotinib metabolite in human plasma. This may diffuse to other tissues where it is oxidized to generate the reactive quinone-imine. Redox cycling of quinone-imines are implicated in a number of drug-related adverse effect and have been shown to produce oxidative stress (Hinson et al., 2004) and covalently modify cellular proteins (Guengerich and MacDonald, 2007; Tang, 2007). This potentially contributes to the clinically observed toxicities.

Little is known about erlotinib-induced Stevens-Johnson syndrome and toxic epidermal necrolysis, but these syndromes are considered immunogenic, are commonly drug-induced, and drugs commonly associated with initiating these toxicities do not share common targets (Khan et al., 2006). Many compounds that are reported to induce Stevens-Johnson syndrome are associated with metabolic activation to form reactive intermediates such as carbamazepine, diclofenac, penicillins, modafinil, acetaminophen, ibuprofen, and phenytoin (Neuman and Nicar, 2007; Locharernkul et al., 2008; Levi et al., 2009).

Erlotinib also contains a terminal alkyne group. The oxidation of terminal alkynes by P450 have been shown to form reactive oxirene and ketene intermediates which can react with water or other cellular nucleophiles, and have been proposed to be involved in inactivation of P450 through formation of protein adducts and through oxidation of the heme group of the P450 enzyme (Ortiz de Montellano and Kunze, 1980; Ortiz de Montellano and Kunze, 1981; Ortiz de Montellano, 1985). We did not see evidence that reactive oxirene or ketene intermediates were released from the enzyme active site or that they were involved in enzyme inactivation. The alkyne group of erlotinib was oxidized by P450 to form a carboxylic acid (a known metabolite (Ling et al., 2006)), but several recombinant P450 enzymes were capable of formation of the

carboxylic acid metabolite and this did not correlate with either formation of glutathione adducts, or with enzyme inactivation (data not shown).

We did not observe erlotinib adducts when a second trapping agent better suited for the expected reactive intermediates generated by alkyne oxidation, N-acetyl lysine, was used. This alone did not sufficiently demonstrate that oxidation of the alkyne was not responsible for the observed CYP3A4/5 inactivation. To address this possibility, the alkyne group of erlotinib was replaced with an ethyl and a cyano group. Both analogs formed glutathione adducts when oxidized by CYP3A4. Additionally, the cyano analog was found to be a time-dependent inhibitor of CYP3A4 demonstrating that enzyme inactivation was not dependent on the alkyne substituent, but we cannot conclude that the alkyne does not act as a second rout for CYP3A4 inactivation.

In summary, the current study identifies erlotinib as a mechanism based inactivator of CYP3A4 and CYP3A5. CYP3A4 is the primary hepatic and intestinal enzyme responsible for the catalysis of reactive erlotinib metabolites, and CYP1A1/2 are primarily responsible for pulmonary adduct formation. Erlotinib bioactivation is proposed to be through the formation of a reactive epoxide and through the formation of a quinone-imine, which may contribute to some of the clinical adverse drug reactions.

Acknowledgments

Scripps manuscript #20415.

DMD Fast Forward. Published on April 9, 2010 as DOI: 10.1124/dmd.109.030361
This article has not been copyedited and formatted. The final version may differ from this version.

References

Bovenschen HJ and Alkemade JA (2009) Erlotinib-induced dermatologic side-effects. *Int J Dermatol* **48:**326-328.

Chou LS, Garey J, Oishi K and Kim E (2006) Managing dermatologic toxicities of epidermal growth factor receptor inhibitors. *Clin Lung Cancer* **8 Suppl 1:**S15-22.

Dahlin DC, Miwa GT, Lu AY and Nelson SD (1984) N-acetyl-p-benzoquinone imine: a cytochrome P-450-mediated oxidation product of acetaminophen. *Proc Natl Acad Sci U S A* **81:**1327-1331.

Dieckhaus CM, Fernandez-Metzler CL, King R, Krolikowski PH and Baillie TA (2005) Negative ion tandem mass spectrometry for the detection of glutathione conjugates. *Chem Res Toxicol* **18:**630-638.

Guengerich FP and MacDonald JS (2007) Applying mechanisms of chemical toxicity to predict drug safety. *Chem Res Toxicol* **20:**344-369.

Hamilton M, Wolf JL, Rusk J, Beard SE, Clark GM, Witt K and Cagnoni PJ (2006) Effects of smoking on the pharmacokinetics of erlotinib. *Clin Cancer Res* **12:**2166-2171.

Hinson JA, Reid AB, McCullough SS and James LP (2004) Acetaminophen-induced hepatotoxicity: role of metabolic activation, reactive oxygen/nitrogen species, and mitochondrial permeability transition. *Drug Metab Rev* **36:**805-822.

Hukkanen J, Pelkonen O, Hakkola J and Raunio H (2002) Expression and regulation of xenobiotic-metabolizing cytochrome P450 (CYP) enzymes in human lung. *Crit Rev Toxicol* **32:**391-411.

Khan FD, Roychowdhury S, Gaspari AA and Svensson CK (2006) Immune response to xenobiotics in the skin: from contact sensitivity to drug allergy. *Expert Opin Drug Metab Toxicol* **2:**261-272.

Levi N, Bastuji-Garin S, Mockenhaupt M, Roujeau JC, Flahault A, Kelly JP, Martin E, Kaufman DW and Maison P (2009) Medications as risk factors of Stevens-Johnson syndrome and toxic epidermal necrolysis in children: a pooled analysis. *Pediatrics* **123:**e297-304.

Li J, Zhao M, He P, Hidalgo M and Baker SD (2007) Differential metabolism of gefitinib and erlotinib by human cytochrome P450 enzymes. *Clin Cancer Res* **13:**3731-3737.

Li X, He Y, Ruiz CH, Koenig M and Cameron MD (2009) Characterization of dasatinib and its structural analogs as CYP3A4 mechanism-based inactivators and the proposed bioactivation pathways. *Drug Metab Dispos* **37:**1242-1250.

Ling J, Johnson KA, Miao Z, Rakhit A, Pantze MP, Hamilton M, Lum BL and Prakash C (2006) Metabolism and excretion of erlotinib, a small molecule inhibitor of epidermal growth factor receptor tyrosine kinase, in healthy male volunteers. *Drug Metab Dispos* **34:**420-426.

Liu V, White DA, Zakowski MF, Travis W, Kris MG, Ginsberg MS, Miller VA and Azzoli CG (2007a) Pulmonary toxicity associated with erlotinib. *Chest* **132:**1042-1044.

Liu W, Makrauer FL, Qamar AA, Janne PA and Odze RD (2007b) Fulminant hepatic failure secondary to erlotinib. *Clin Gastroenterol Hepatol* **5:**917-920.

Locharernkul C, Loplumlert J, Limotai C, Korkij W, Desudchit T, Tongkobpetch S, Kangwanshiratada O, Hirankarn N, Suphapeetiporn K and Shotelersuk V (2008) Carbamazepine and phenytoin induced Stevens-Johnson syndrome is associated with HLA-B*1502 allele in Thai population. *Epilepsia* **49:**2087-2091.

Lubbe J, Masouye I and Dietrich PY (2008) Generalized xerotic dermatitis with neutrophilic spongiosis induced by erlotinib (Tarceva). *Dermatology* **216:**247-249.

Makris D, Scherpereel A, Copin MC, Colin G, Brun L, Lafitte JJ and Marquette CH (2007) Fatal interstitial lung disease associated with oral erlotinib therapy for lung cancer. *BMC Cancer* **7:**150.

Moore MJ, Goldstein D, Hamm J, Figer A, Hecht JR, Gallinger S, Au HJ, Murawa P, Walde D, Wolff RA, Campos D, Lim R, Ding K, Clark G, Voskoglou-Nomikos T, Ptasynski M and Parulekar W (2007) Erlotinib plus gemcitabine compared with gemcitabine alone in patients with advanced pancreatic cancer: a phase III trial of the National Cancer Institute of Canada Clinical Trials Group. *J Clin Oncol* **25:**1960-1966.

Neuman M and Nicar M (2007) Apoptosis in ibuprofen-induced Stevens-Johnson syndrome. *Transl Res* **149:**254-259.

Ortiz de Montellano PR (1985) *Alkenes and alkynes.* Academic Press, New York.

Ortiz de Montellano PR and Kunze KL (1980) Self-catalyzed inactivation of hepatic cytochrome P-450 by ethynyl substrates. *J Biol Chem* **255:**5578-5585.

Ortiz de Montellano PR and Kunze KL (1981) Shift of the acetylenic hydrogen during chemical and enzymatic oxidation of the biphenylacetylene triple bond. *Arch Biochem Biophys* **209:**710-712.

OSI Pharmaceuticals and Genentech (2008) Dear Healthcare Professional.

Pellegrinotti M, Fimognari FL, Franco A, Repetto L and Pastorelli R (2009) Erlotinib-induced hepatitis complicated by fatal lactic acidosis in an elderly man with lung cancer. *Ann Pharmacother* **43:**542-545.

Perloff ES, Mason AK, Dehal SS, Blanchard AP, Morgan L, Ho T, Dandeneau A, Crocker RM, Chandler CM, Boily N, Crespi CL and Stresser DM (2009) Validation of cytochrome P450 time-dependent inhibition assays: a two-time point IC50 shift approach facilitates kinact assay design. *Xenobiotica* **39:**99-112.

Ramanarayanan J and Scarpace SL (2007) Acute drug induced hepatitis due to erlotinib. *JOP* **8:**39-43.

Rudin CM, Liu W, Desai A, Karrison T, Jiang X, Janisch L, Das S, Ramirez J, Poonkuzhali B, Schuetz E, Fackenthal DL, Chen P, Armstrong DK, Brahmer JR, Fleming GF, Vokes EE, Carducci MA and Ratain MJ (2008) Pharmacogenomic and pharmacokinetic determinants of erlotinib toxicity. *J Clin Oncol* **26:**1119-1127.

Saif MW (2008) Erlotinib-induced acute hepatitis in a patient with pancreatic cancer. *Clin Adv Hematol Oncol* **6:**191-199.

Siegel-Lakhai WS, Beijnen JH and Schellens JH (2005) Current knowledge and future directions of the selective epidermal growth factor receptor inhibitors erlotinib (Tarceva) and gefitinib (Iressa). *Oncologist* **10:**579-589.

Takano T, Ohe Y, Kusumoto M, Tateishi U, Yamamoto S, Nokihara H, Yamamoto N, Sekine I, Kunitoh H, Tamura T, Kodama T and Saijo N (2004) Risk factors for interstitial lung disease and predictive factors for tumor response in patients with advanced non-small cell lung cancer treated with gefitinib. *Lung Cancer* **45:**93-104.

Tang PA, Tsao MS and Moore MJ (2006) A review of erlotinib and its clinical use. *Expert Opin Pharmacother* **7:**177-193.

Tang W (2007) Drug metabolite profiling and elucidation of drug-induced hepatotoxicity. *Expert Opin Drug Metab Toxicol* **3:**407-420.

Thum T, Erpenbeck VJ, Moeller J, Hohlfeld JM, Krug N and Borlak J (2006) Expression of xenobiotic metabolizing enzymes in different lung compartments of smokers and nonsmokers. *Environ Health Perspect* **114:**1655-1661.

DMD Fast Forward. Published on April 9, 2010 as DOI: 10.1124/dmd.109.030361
This article has not been copyedited and formatted. The final version may differ from this version.

Legend for Scheme

Scheme 1. Proposed mechanism of erlotinib-glutathione adduct formation.

Legends for Figures

Fig.1. Time- and Concentration-dependent inactivation of CYP3A4 by erlotinib. Incubations containing 0.5 mg/ml HLM and 1 mM NADPH in 100 mM phosphate buffer, pH 7.4, were incubated with the following erlotinib concentrations: 0, 5, 10, 20, and 40 μM. (A) At the indicated time points, the remaining CYP3A4 activity was measured by a midazolam hydroxylation assay. Each point represents the mean of triplicate incubation. The observed inactivation rate constants, K_{obs}, were calculated from the slopes of the regression lines in A. (B) The hyperbolic plot of K_{obs} versus erlotinib concentration was used to calculate kinetic constants. Potential preservation of CYP3A4 activity by the addition of 5 mM glutathione or 1000 units of superoxide dismutase and catalase to incubations containing 0.5 mg/ml HLM, 1 mM NADPH, and 20 μM erlotinib was evaluated (C).

Fig.2. Formation of erlotinib-glutathione adducts. (A) Erlotinib-glutathione adducts were detected in one-hour incubations containing 2 mg/ml HLM, 1 mM NADPH, 40 μM erlotinib and 5 mM glutathione, in 100 mM phosphate buffer, pH 7.4. Parallel incubations to those in (A) were prepared without glutathione and after one hour the solution was directly applied to a solid-phase extraction column. The column was washed with twenty bed volumes of water and eluted with acetonitrile. The acetonitrile was evaporated and erlotinib and its metabolites were reconstituted in phosphate buffer with 5 mM glutathione and incubated at 37°C for 4 hours (B).

DMD Fast Forward. Published on April 9, 2010 as DOI: 10.1124/dmd.109.030361
This article has not been copyedited and formatted. The final version may differ from this version.

Fig.3. MS/MS spectrum of the MH+ ion m/z 715.3 of ELR-G5. The origins of the characterized ions are as indicated.

Fig.4. H-NMR spectrum of ERL-G6.

Fig.5. Effect of NADPH and superoxide dismutase plus catalase on the formation rate of ERL-G6 in recombinant P450 incubations. All incubations had 100 pmol/ml P450, 5 mM glutathione, and 20 μM erlotinib in 100 mM phosphate buffer, pH 7.4. Filled bars contained 1 mM NADPH, open bars did not have NADPH, and hashed bars had 1 mM NADPH plus 1000 units of superoxide dismutase and 1000 units of catalase.

Fig.6. ERL-G5 formation by recombinant P450 enzymes. ERL-G5 generation was compared in incubations containing 100 pmol/ml P450, 1 mM NADPH, 5 mM glutathione, and 40 μM erlotinib (A). Relative ELR-G5 concentration was determined by comparison of the peak area of ELR-G5 to an internal standard. The enzyme activities were expressed as the percentage of CYP3A4 activity and are an average of two measurements. Correlation analysis of ERL-G5 formation to formation of the *para*-hydroxyaniline metabolite in HLM and recombinant P450 is shown in plot B.

Fig.7. CYP3A and CYP1A inhibition on ERL-G5 formation. (A) ERL-G5 production was measured in incubations where the CYP3A inhibitor ketoconazole (1 μM) was added to human pulmonary (smoker), intestinal, and hepatic microsomes. (B) Inhibition of CYP3A (1 μM ketoconazole) and CYP1A (20 μM α-naphthoflavone) was tested in incubations containing pulmonary microsomes from smokers (S) and non-smokers (NS). All incubations contained 2 mg/ml microsomal protein, 40 μM erlotinib, 5 mM glutathione, and 1 mM NADPH in 100 mM phosphate buffer, pH 7.4. The values were an average of two replicates.

DMD Fast Forward. Published on April 9, 2010 as DOI: 10.1124/dmd.109.030361
This article has not been copyedited and formatted. The final version may differ from this version.

Fig.8. Influence of human microsomal epoxide hydrolase on the formation of ERL-G5. The addition of 1 mg/ml human microsomal epoxide hydrolase was evaluated in incubations of HLM, and recombinant CYP3A4 and CYP1A1. Incubations containing 2 mg/ml HLM or 100 pmol/ml recombinant P450, 1 mM NADPH, 5 mM glutathione, and 40 μM erlotinib in 100 mM phosphate buffer, pH 7.4. The values were an average of two replicates.

DMD Fast Forward. Published on April 9, 2010 as DOI: 10.1124/dmd.109.030361
This article has not been copyedited and formatted. The final version may differ from this version.

Table 1. Erlotinib tissue distribution.

	tissue erlotinib concentration (μM)			
	Plasma	Brain	Liver	Lung
erlotinib	5.4 +/- 1.6	0.37 +/- 0.14	14.7 +/- 2.8	5.0 +/- 1.2

2 hours after a single 10 mg/kg oral dose in C57Bl/6 mice
Tissues were not perfused to assure erlotinib was not washed out during perfusion.

DMD Fast Forward. Published on April 9, 2010 as DOI: 10.1124/dmd.109.030361
This article has not been copyedited and formatted. The final version may differ from this version.

Scheme 1.

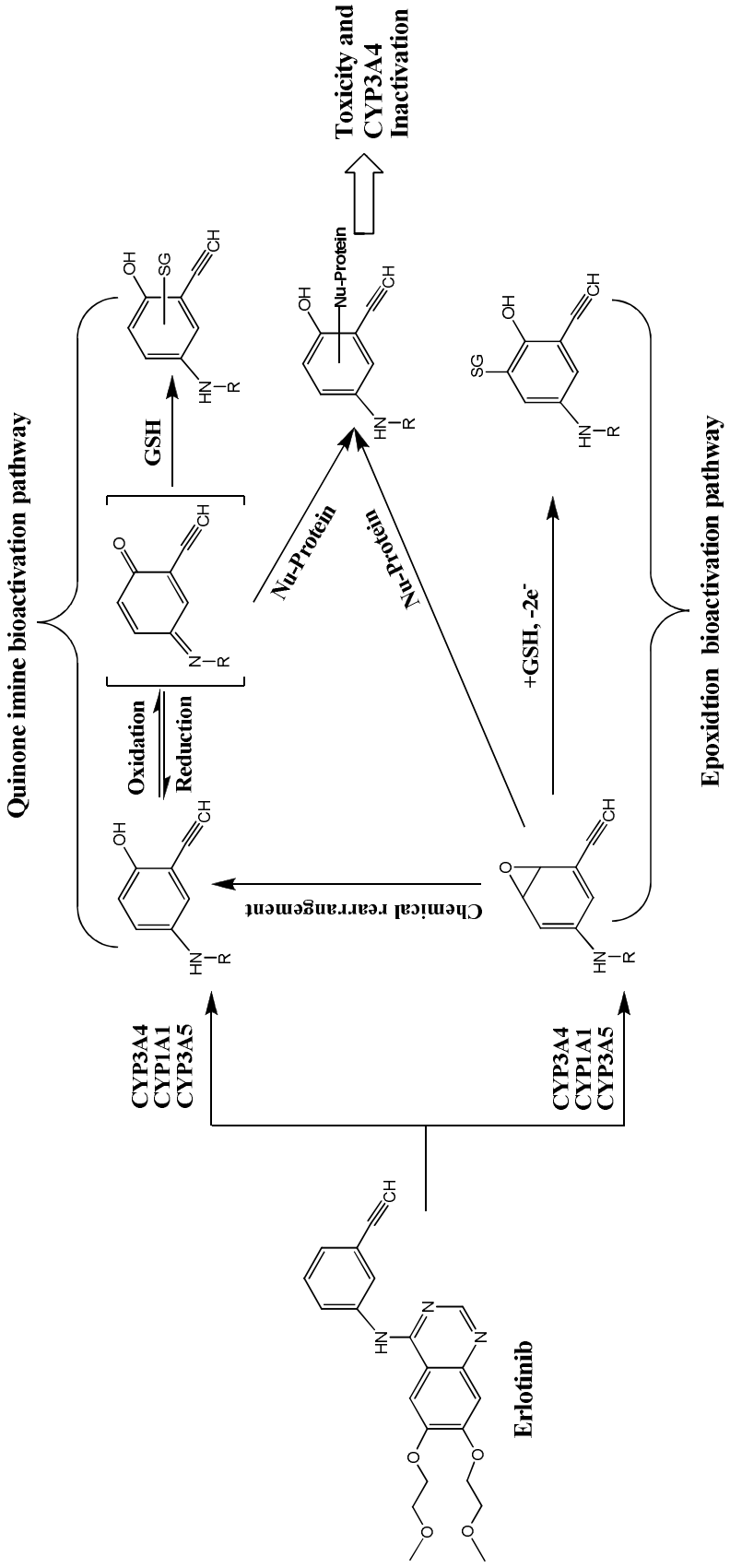

Fig 1

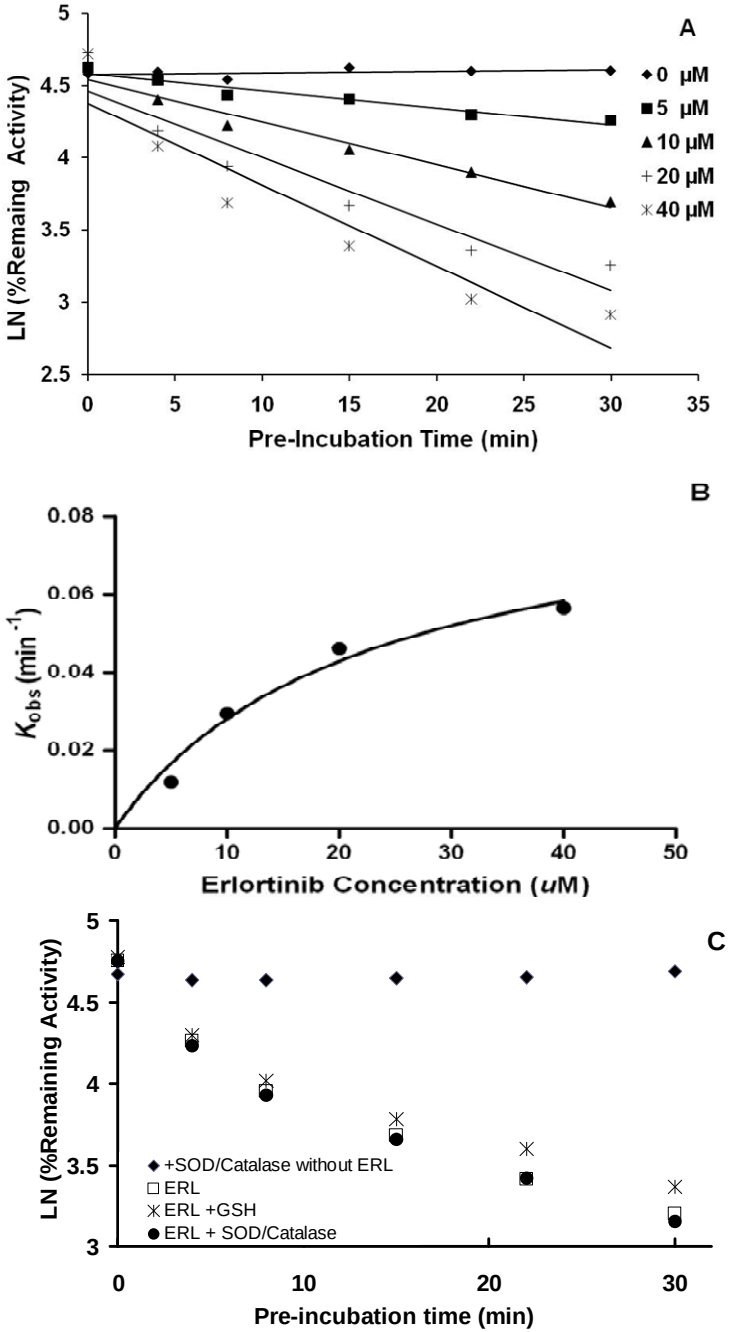

Fig 2

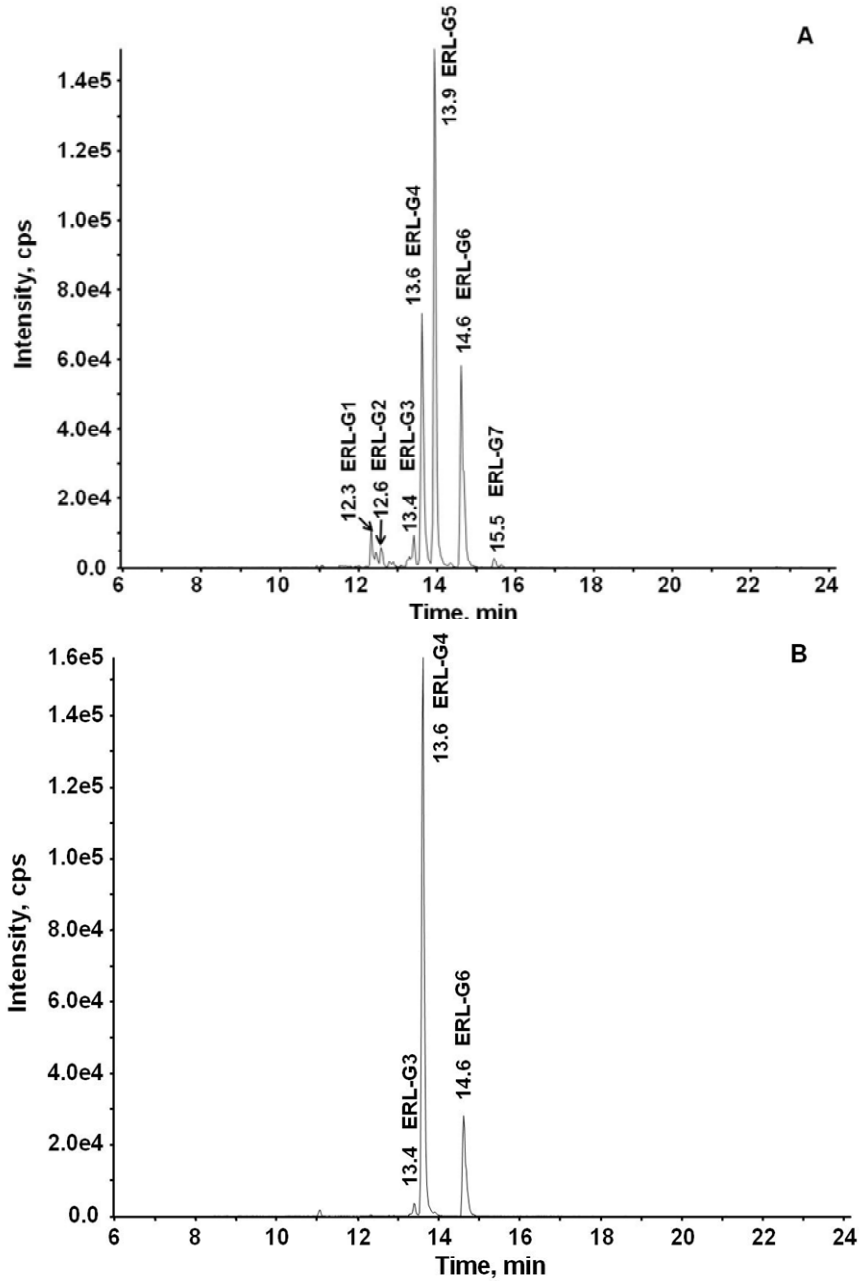

Fig 3

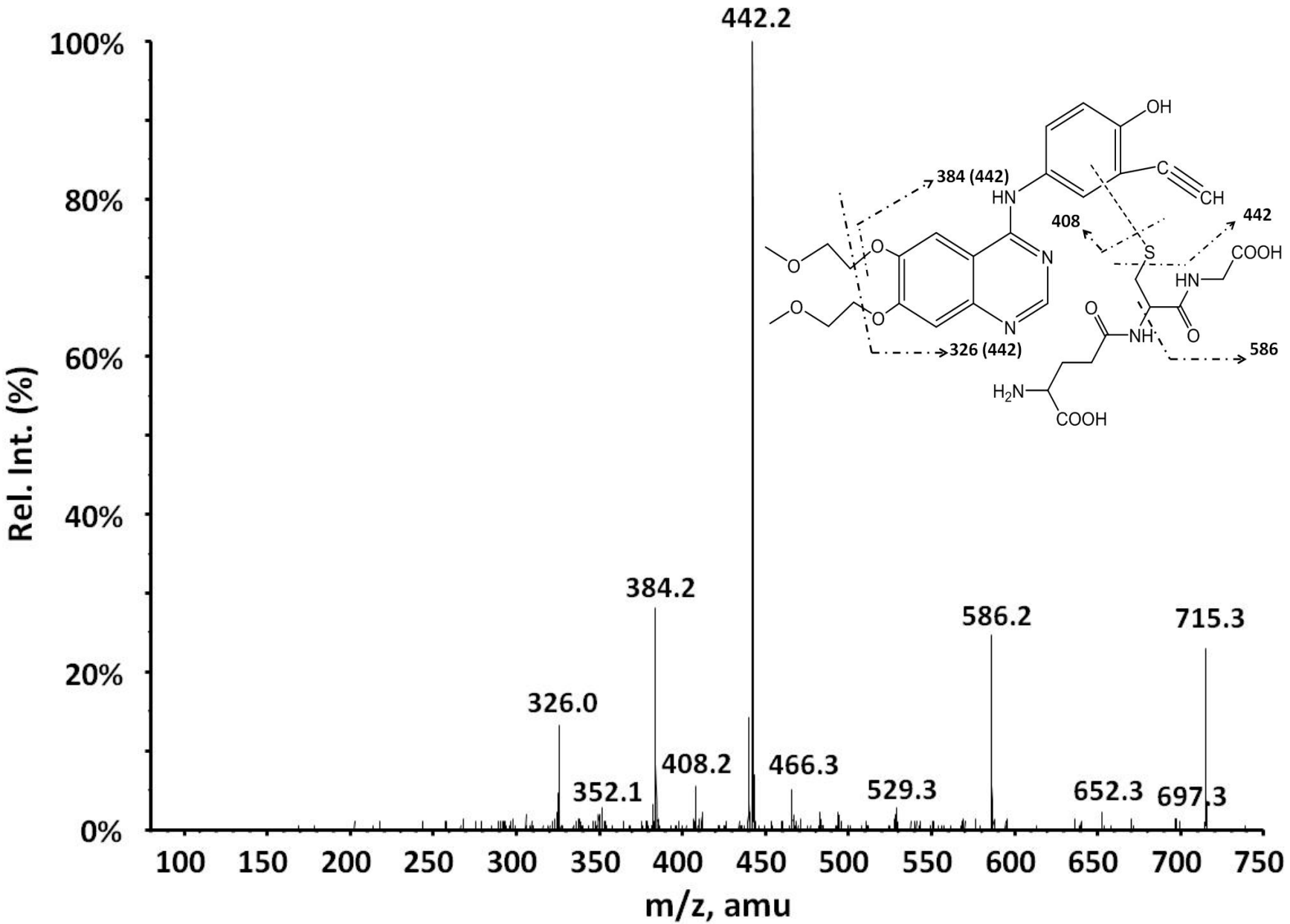

Fig 4

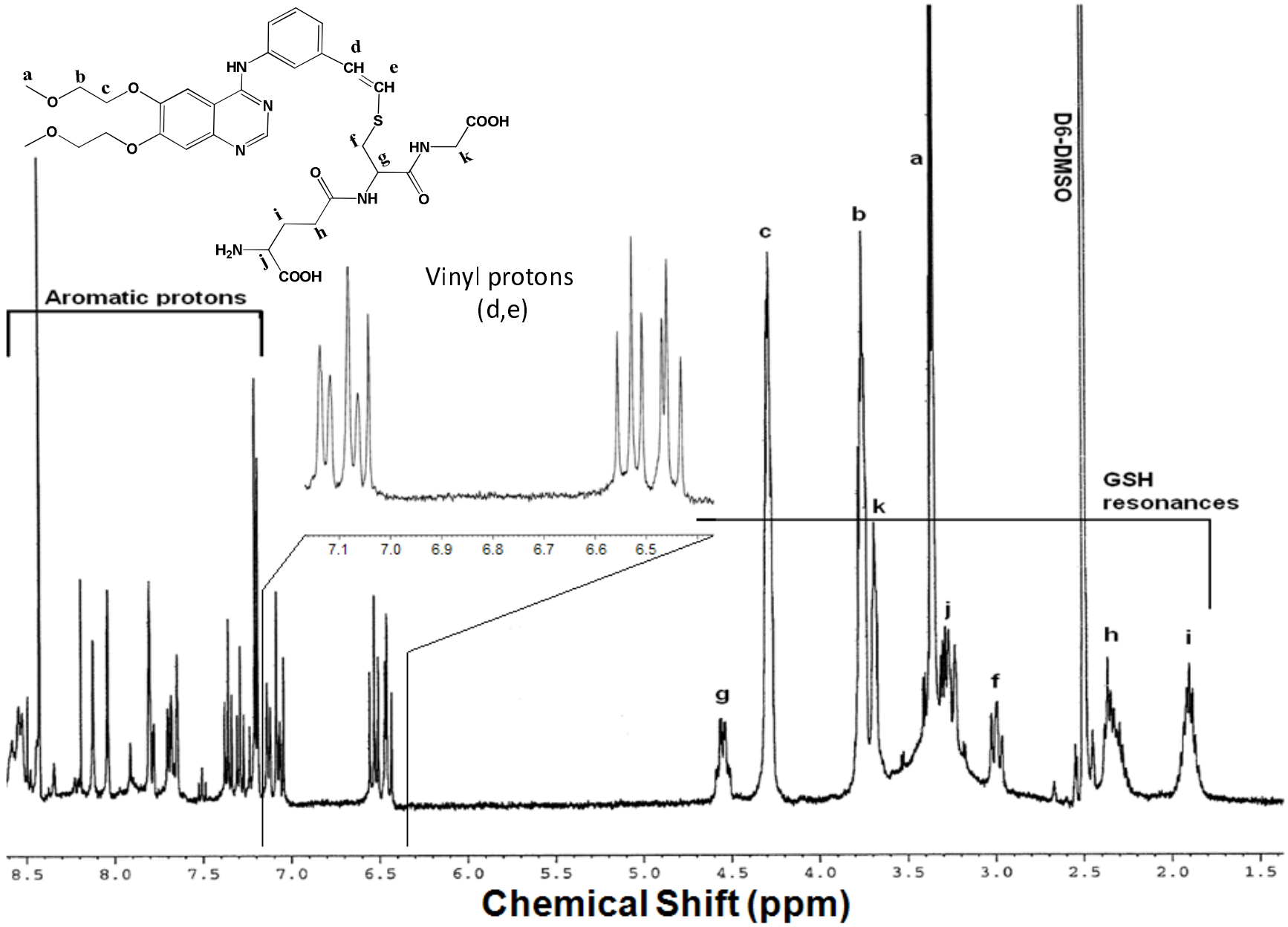

Fig 5

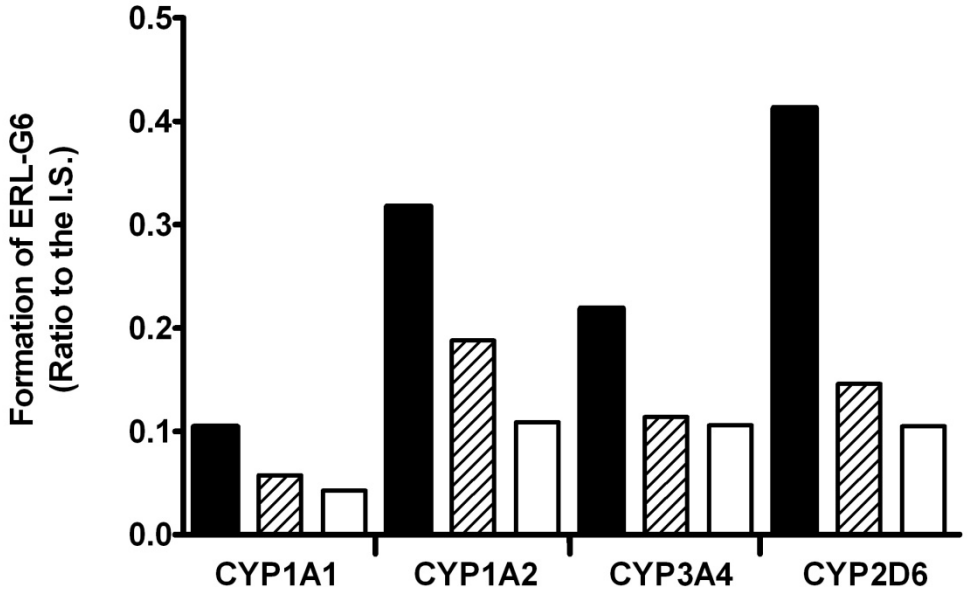

Fig 6

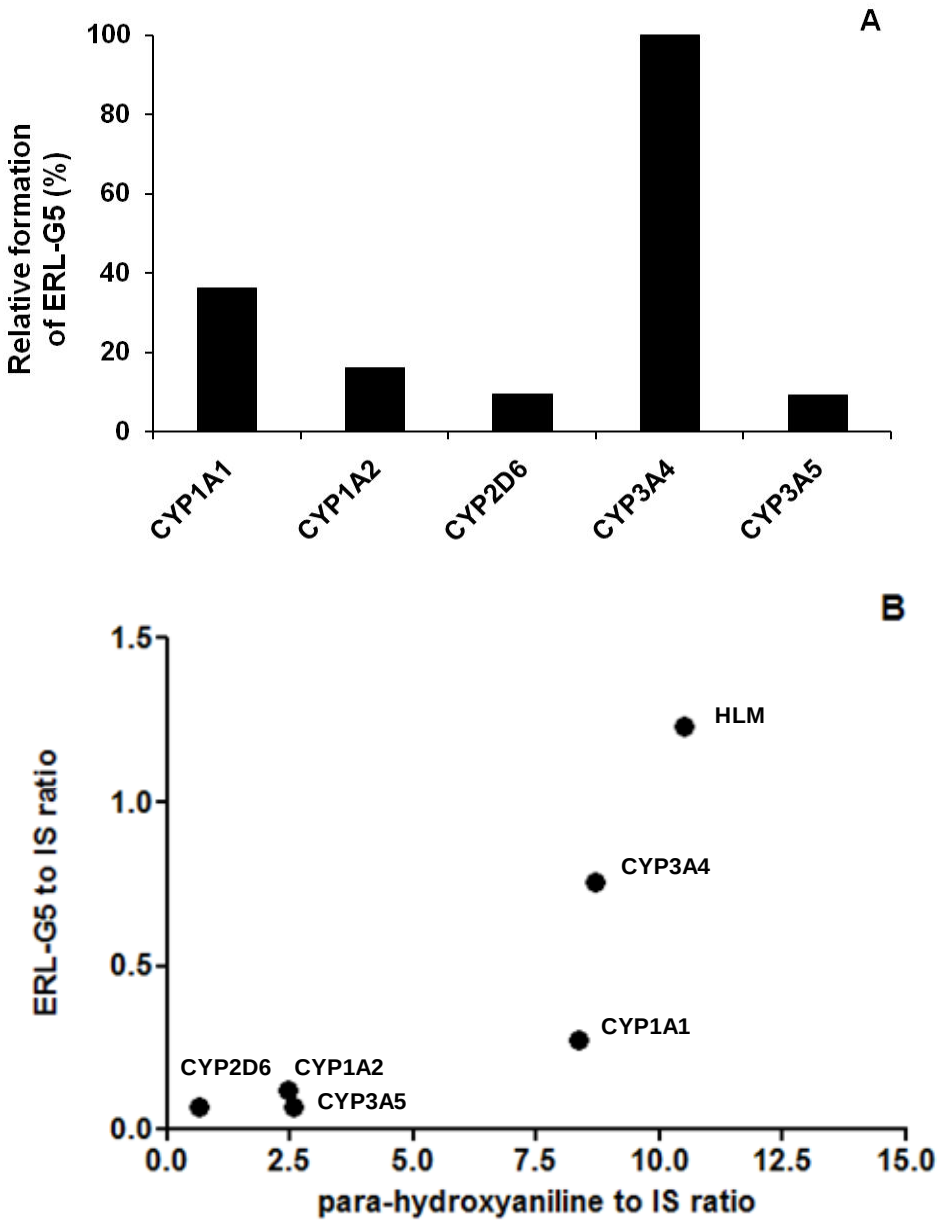

Fig 7

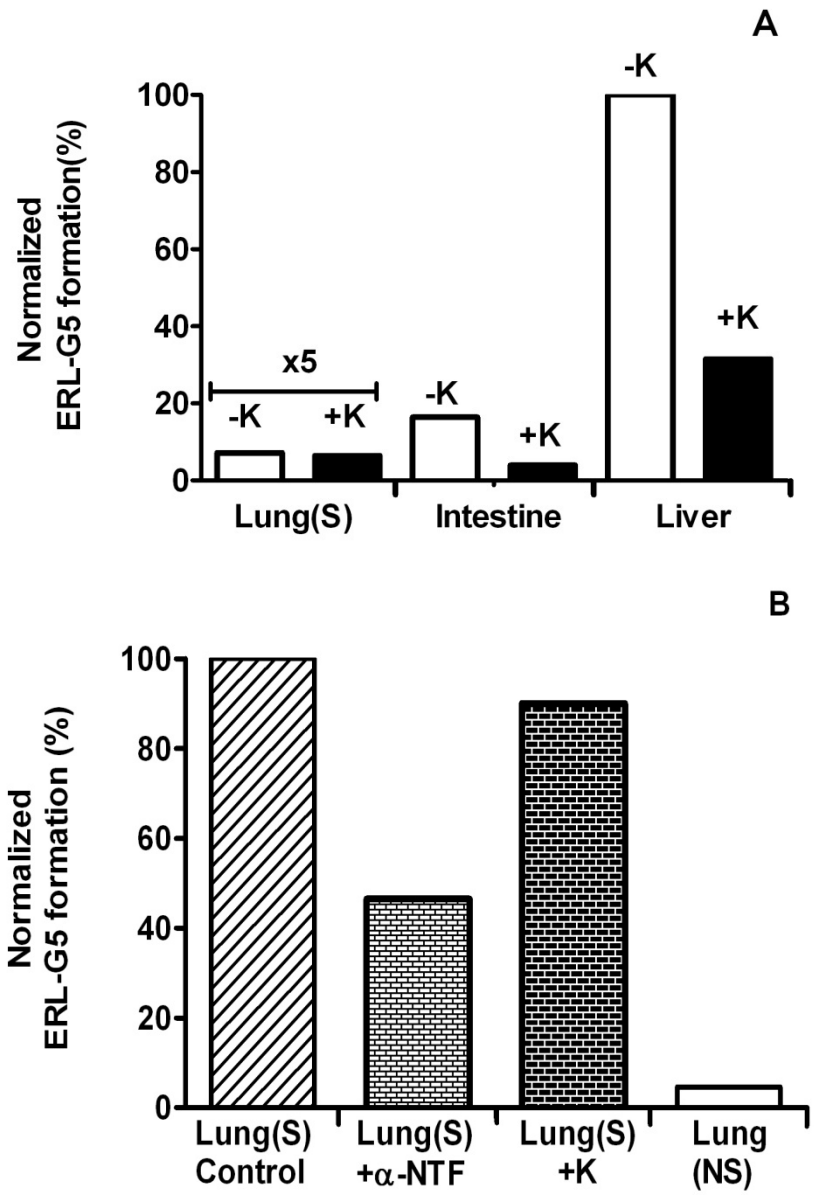

Fig 8